Fish & Shellfish Immunology 51 (2016) 291–302

Contents lists available at ScienceDirect

Fish & Shellfish Immunology

journal homepage: www.elsevier.com/locate/fsi

Full length article

# Identification and molecular characterization of peroxiredoxin 6 from Japanese eel (*Anguilla japonica*) revealing its potent antioxidant properties and putative immune relevancy

Thanthrige Thiunuwan Priyathilaka [a, b], Yucheol Kim [a, b], H.M.V. Udayantha [a, b], Seongdo Lee [a, b], H.M.L.P.B. Herath [a, b], H.H. Chaminda Lakmal [a], Don Anushka Sandaruwan Elvitigala [a, b], Navaneethaiyer Umasuthan [a, b], G.I. Godahewa [a, b], Seong Il Kang [a, b], Hyung Bok Jeong [b], Shin Kwon Kim [c], Dae Jung Kim [c], Bong Soo Lim [b, *]

[a] Department of Marine Life Sciences, School of Marine Biomedical Sciences, Jeju National University, Jeju Self-Governing Province 690-756, Republic of Korea
[b] Fish Vaccine Research Center, Jeju National University, Jeju Special Self-Governing Province 695-965, Republic of Korea
[c] New Strategy Research Center, National Fisheries Research and Development Institute, Busan 619-705, Republic of Korea

ARTICLE INFO

*Article history:*
Received 5 August 2015
Received in revised form
3 December 2015
Accepted 11 December 2015
Available online 18 February 2016

*Keywords:*
Peroxiredoxin 6
*Anguilla japonica*
Antioxidant
Oxidative stress

ABSTRACT

Peroxiredoxins (Prdx) are thiol specific antioxidant enzymes that play a pivotal role in cellular oxidative stress by reducing toxic peroxide compounds into nontoxic products. In this study, we identified and characterized a peroxiredoxin 6 counterpart from Japanese eel (*Anguilla japonica*) (AjPrdx6) at molecular, transcriptional and protein level. The identified full-length coding sequence of *AjPrdx6* (669 bp) coded for a polypeptide of 223 aa residues (24.9 kDa). Deduced protein of AjPrdx6 showed analogy to characteristic structural features of 1-cysteine peroxiredoxin sub-family. According to the topology of the generated phylogenetic reconstruction AjPrdx6 showed closest evolutionary relationship with *Salmo salar*. As detected by Quantitative real time PCR (qPCR), *AjPrdx6* mRNA was constitutively expressed in all the tissues examined. Upon the immune challenges with *Edwardsiella tarda*, lipopolysaccharides and poly-inosinic:polycytidylic acid, expression of *AjPrdx6* mRNA transcripts were significantly induced. The general functional properties of Prdx6 were confirmed using purified recombinant AjPrdx6 protein by deciphering its potent protective effects on cultured vero cells (kidney epithelial cell from an African green monkey) against $H_2O_2$-induced oxidative stress and protection against oxidative DNA damage elicited by mixed function oxidative (MFO) system. Altogether, our findings suggest that AjPrdx6 is a potent antioxidant protein in Japanese eels and its putative immune relevancy in pathogen stress mounted by live-bacteria or pathogen associated molecular patterns (PAMPs).



## 1. Introduction

Reactive oxygen species (ROS) contain chemically reactive oxygen molecules which are resulted as the byproducts of respiration in aerobic organisms. Minor concentrations of ROS are mandatory for the normal cellular functions, including intracellular signal transduction, regulation of gene expression, host defense against pathogenic infections and so on [1–3]. However, excessive production of ROS might cause accumulation of free oxygen intermediates in intracellular environment, resulting wide array of adverse effects, such as nucleic acid damage, protein oxidation, lipid peroxidation and modification of lipoproteins [3–6]. Hence, maintenance of optimum intracellular ROS level is vital for regulation of routine cellular functions. Antioxidants are known to play a critical role in regulating the ROS level by detoxifying deleterious oxygen intermediates without disrupting the normal cellular functions. To date, several types of enzymatic and non-enzymatic antioxidants have been identified in living organisms [3].

Prdxs are a large family of thiol peroxidases, which play a pivotal role in cellular oxidative stress by reducing the hydrogen peroxide,

* Corresponding author.
*E-mail addresses:* djkim4128@korea.kr (D.J. Kim), bslim@jejunu.ac.kr (B.S. Lim).

http://dx.doi.org/10.1016/j.fsi.2015.12.012
1050-4648/

peroxynitrite and various kinds of organic hydroperoxides into nontoxic forms [7–10]. Typically, Prdxs can be identified in all kingdoms of life including plants, animals and yeasts [8]. Recently, six different isoforms of Prdxs (Prdx1–Prdx6) which are encoded by multiple distinct genes have been discovered in mammals [11]. The six members of the Prdx family are mainly divided into 1-cysteine Prdx (1-Cys Prdx), and 2-Cys Prdx classes depending on the number of catalytically active cysteine residues involved in catalysis [8,12–14]. Considering the structural features and the catalysis mechanism, the 2-Cys Prdx class is further sub-divided into typical 2-Cys Prdx and atypical 2-Cys Prdx sub-groups. All the members of typical 2-Cys Prdx (Prdx1-Prdx4) subgroup are comprised with two conserved catalytic cysteine residues at both N- and C-termini, named as peroxidatic cysteine (Cys-SpH) and resolving cysteine ($CyS_R$-SH) respectively [7,8,12,15]. The atypical 2-Cys Prdx (Prdx5) contains only the conserved Cys-SpH, however one additional non-conserved cysteine residue is required for its catalytic cycle [7,8]. Apart from the 2-Cys Prdxs, 1-Cys Prdx subgroup requires only one cysteine residue for its peroxdatic catalytic cycle [8].

The Prdx6 is referred as a bi-functional enzyme due to its glutathione-peroxidase activity and phospholipase A2 (PLA2) activity [16,17]. To date, Prdx6 has extensively been studied in mammals including human (*homo sapiens*) [16,18,19], rat (*Rattus norvegicus*) [20], mouse (*Mus musculus*) [21,22] and cattle (*Bos taurus*) [23], although it has been characterized in several fish species (*Scophthalmus maximus* [24], *Oplegnathus fasciatus* [25], and *Sparus aurata* [11]), arthropods (*Eriocheir sinensis* [26]) and mollusks (*Haliotis discus discus* [27] and *Crassostrea gigas*) [28]. Prdx6 is the only member of 1-Cys Prdx sub-family, which contains a single conserved catalytically active cysteine residue at N-terminus catalytic center (PVCTTE) for the peroxidase activity [9,29,30]. *Prdx6* is ubiquitously distributed in all major tissues, while abundantly expressed in tissues that are vulnerable to oxidative stress [24,25,30–32]. Expression of *Prdx6* markedly modulated upon several stimuli including live bacteria [24,26], virus [25,27], PAMPs [24,25], chemicals ($H_2O_2$) [33], thermal stress [33,34], and environmental pollutants [28] in several organisms. Number of studies demonstrated that Prdx6 exerts its extensive antioxidant properties *in vivo* [22,35]. Moreover, functional activities of purified recombinant Prdx6 (rPrdx6) have been determined in some of the species. It has been shown a significant protective effect of rPrdx6 on cultured cells against $H_2O_2$ mediated oxidative stress [24,27]. Furthermore, some of the studies showed that the rPrdx6s effectively inhibit the conversion of supercoiled DNA into nicked form [25,33,36] and protection of genomic DNA against oxidative stress [27].

Japanese eel is a most popular and economically important aquaculture fish species in Korea and Japan, which is considered as a high priced fish in the market. However, due to several pathogenic infections, especially caused by bacterial pathogens, the eel aquaculture industry is being faced to vast economic losses [37,38]. Therefore, studies on adaptive and innate immune components and their function against pathogenic stress is really important for developing the disease management strategies. In this study, we identified a peroxiredoxin 6 homolog from Japanese eel, and designated *AjPrdx6*. Further the transcriptional modulations of *AjPrdx6* upon live bacteria and pathogen-derived mitogens were determined using qPCR in liver and spleen tissues. Moreover, antioxidant properties of recombinant AjPrdx6 were determined.

## 2. Materials and methods

### 2.1. Identification of AjPrdx6 cDNA sequence

The cDNA sequence of *AjPrdx6* with prominent homology to known *Prdx6* was identified using the Basic Local Alignment Search Tool (BLAST; http://blast.ncbi.nlm.nih.gov/) from a previously constructed *Anguilla japonica* transcriptomic database by GL-FLX titanium DNA sequencing technology (Roche 454 genome sequencer FLX systems; Macrogen, Republic of Korea).

### 2.2. In silico analysis

The putative open reading frame (ORF) and deduced amino acid sequence along with several physiochemical properties of AjPrdx6 was determined using UGENE software [39] and ExPASy ProtParam online tool (http://web.expasy.org/protparam/). The anticipated domain structure of AjPrdx6 protein was determined by the Simple Modular Architecture Research Tool (SMART) (http://smart.embl-heidelberg.de/). ClustalW2 (http://www.ebi.ac.uk/Tools/msa/clustalw2/) and EMBOSS Needle (http://www.ebi.ac.uk/Tools/psa/emboss_needle/) online servers were used to perform the multiple sequence alignment and the pairwise sequence alignment respectively. A phylogenetic tree was generated by the neighbor joining (NJ) method using Molecular Evolutionary Genetic Analysis (MEGA) software version 5.0, validated by 1000 bootstrap replications. Furthermore, 3D structural homology model of AjPrdx6 was predicted by ITASSER online server and visualized using PyMOL molecular graphic software (http://www.pymol.org/).

### 2.3. Experimental animals and tissue isolation

Healthy Japanese eels with body weight of around 100 g were reared in 400 L tanks with aerated fresh water at a temperature of 24 ± 1 °C in the Fish Vaccine Research Center, Jeju National University, Republic of Korea. All the Japanese eels were acclimatized to the laboratory conditions for three weeks prior to the experiment.

To evaluate the tissue specific expression of *AjPrdx6*, brain, liver, kidney, head kidney, spleen, heart, gills, intestine, skin, muscles and gonad were isolated from five healthy animals. All the tissues were snap frozen in liquid nitrogen and subsequently stored at −80 °C until RNA extraction.

### 2.4. Immune challenge experiment

In order to determine the immune modulatory properties of *AjPrdx6* upon pathogenic condition, four groups of healthy Japanese eels were subjected to the time-course immune challenge experiments. For pathogen-derived mitogen experiment, 100 μL of lipopolysaccharide (LPS) suspended in phosphate buffered saline (PBS) (2 μg/μL; *Escherichia coli* 055:B5, Sigma) and 100 μL of polyinosinic:polycytidylic (Poly I:C) acid in PBS (2 μg/μL, Sigma) were intraperitonealy injected to each fish from two separate fish groups respectively. The Gram negative bacterial pathogen; *Edwardsiella tarda* was inoculated to the 100 mL of brain heart infusion (BHI) broth supplemented with 1% sodium chloride and incubated in shaking incubator at 25 °C for 10 h. Thereafter, bacterial cells were harvested by centrifugation at 3000 rpm at 4 °C for 30 min. Harvested cells were subsequently resuspended in PBS, and then diluted to desired concentration. Then each fish from another Japanese eel group was subjected to the intraperitoneal injection of 100 μL *E. tarda* in PBS ($1 \times 10^7$ CFU/mL). For control group, 100 μL of PBS was intraperitonealy injected. Fish were sacrificed at 3 h, 6 h, 12 h, 24 h, 48 h and 72 h post-injection (p.i.) periods, and liver and spleen samples were collected as described in Section 2.3.

### 2.5. RNA extraction

Total RNA was extracted from collected tissues (Section 2.3 and 2.4) using RNAiso plus Total RNA extraction reagent (TaKaRa,

Japan). Extracted RNA was subjected to the DNase treatment (Promega, USA). Briefly, a 10 μL reaction was carried out with 8 μL of extracted RNA, 1 μL of RQ1 RNase-free DNase (1U) and 1 μL of RQ1 RNase-free DNase 10 × reaction buffer. Mixture was incubated at 37 °C for 30 min. After incubation, 1 μL of RQ1 DNase stop solution was added to terminate the reaction and reaction mixture was subsequently incubated at 65 °C for 10 min. Concentration at 260 nm and absorbance ratio (260/280) of extracted RNA was determined before and after the DNase treatment using Nanodrop 2000C spectrophotometer (Thermo Scientific, USA). Moreover, 1 μL of each RNA sample (before and after the DNase treatment) was analyzed on 1% agarose gel stained with ethidium bromide and rest of the samples were stored at −80 °C until use in further analysis.

### 2.6. Expression analysis of AjPrdx6 by qPCR

Expression profile of *AjPrdx6* in different tissues from un-challenged animal group and challenged animal group was investigated by qPCR using the TaKaRa TP850 Thermal Cycler Dice™ Real Time System (TaKaRa, Japan). The qPCR experiment was performed using TOPreal™ One-step RT qPCR kit (SYBR Green) (Enzynomics, Korea). Briefly, the qPCR was carried out in 15 μL total reaction mixture containing, 5.75 μL of template RNA (20 ng) in nuclease free water, 0.75 μL of TOPreal™ One-step RT qPCR Enzyme MIX, 7.5 μL of 2 × TOPreal™ One-step RT qPCR Reaction MIX and 0.5 μL of each primers (10 pmol/μL) (Table 1). The qPCR thermal profile was as follows, hold at 50 °C for 30 min, initial denaturation at 95 °C for 10 min, 45 cycles of 95 °C for 5 s, 60 °C for 10 s, 72 °C for 30 s, and a single cycle of 95 °C 15 s, 60 °C 30 s and 95 °C 15 s. The *Anguilla japonica* Elongation Factor 1-Alpha (*AjEF1-a*) (GeneBank accession no: AB593812) was amplified as an internal control gene using the same qPCR thermal profile. In order to determine the qPCR specificity, the dissociation curves were analyzed; thereafter relative mRNA expression of the *AjPrdx6* was determined according to the Livak ($2^{-\Delta\Delta CT}$) method [40]. In tissue specific distribution analysis, the expression level of *AjPrdx6* in spleen was considered as the basal value. The fold differences of *AjPrdx6* expression in the challenged groups were calculated relative to the un-injected control group (0 h). All the data were collected from five individual samples and presented as mean standard error (SE) of five replicates (n = 5).

### 2.7. Construction of expression vector

Previous experimental evidences demonstrated that the Prdx6 exerted its potent antioxidant activity against oxidative stress. In order to determine whether the antioxidant properties of AjPrdx6, recombinant AjPrdx6 (designated as rAjPrdx6) was expressed as a fusion protein with the maltose binding protein (MBP). The cDNA was synthesized from total RNA extracted from Japanese eel liver tissues (Section 2.3 and 2.5) using Maxime RT PreMix Kit (iNtRON BIOTECHNOLOGY, Korea) following the vendor's protocol. The ORF of *AjPrdx6* was amplified using target specific primers with the restriction sites of *Eco*RI and *Hind*III (Table 1). The Polymerase Chain Reaction (PCR) was performed in TaKaRa thermal cycler Dice™ Touch. Briefly, a 50 μL reaction was carried out with 5 μL of template cDNA, 5 μL of 10 × PCR buffer, 4 μL of dNTP mixture (2.5 mM each), 2 μL of each forward and reverse primer (10 pmol), 0.5 μL of T&I™ Prime Taq Polymerase (5 Units/μL) (Tech & Innovation, Korea) and nuclease free water. The PCR thermal profile was as follows; initial denaturation at 95 °C for 3 min, 35 cycles of 95 °C for 30 s, 55 °C for 30 s, 72 °C for 1 min and final extension at 72 °C for 3 min. Thereafter, purified PCR product was digested with *Eco*RI and *Hind*III along with the pMAL-c2X vector. Then, each digested PCR product and vector were analyzed on the 1% agarose gel and excised for purification using AccuPrep® PCR Purification Kit (Bioneer, Korea), and subsequently ligated into the pMAL-c2X vector. The recombinant pMAL-c2X/AjPrdx6 was transformed into the *Escherichia coli* (*E.coli*) DH5α competent cells and sequenced. Sequence confirmed recombinant pMAL-c2X/AjPrdx6 construct was transformed into *E. coli* BL21 (DE3) competent cells.

### 2.8. Overexpression and purification of rAjPrdx6

The rAjPrdx6 fusion protein was overexpressed in *E. coli* BL21 (DE3) cells using isopropy-b-thiogalactopyranoside (IPTG) induction. In brief, transformed *E. coli* BL21 (DE3) cells were grown in 500 mL of LB broth supplemented with ampicillin (100 μg/mL) and glucose (0.2%) at 37 °C in a shaking incubator until the optical density at 600 nm ($OD_{600}$) reached 0.5. Thereafter, expression of rAjPrdx6 fusion protein was induced by IPTG (final concentration of 0.5 mM) and culture was further incubated at 20 °C for 8 h with shaking. Then, cells were harvested by centrifugation (1200 *g* for 30 min at 4 °C for 30 min) and subsequently resuspended in column buffer (20 mM Tris-HCL, pH 7.4 and 200 mM NaCl) and stored at −20 °C. The harvested cells were lysed by cold-sonication and lysate was immediately subjected to the centrifugation at 9000 *g* at 4 °C for 30 min. Using the pMAL™ protein fusion and purification system, the recombinant AjPrdx6 protein was purified according to the manufactures' instruction (New England BioLabs, USA). Finally, concentration of purified recombinant protein was determined by Bradford method [41]. Moreover, resultant protein was assayed using the 12% SDS-PAGE along with the standard molecular size protein marker and visualized with coomassie brilliant blue R250.

### 2.9. Cell culture

The vero (kidney epithelial cells from an African green monkey) cells from an established cell culture were used for cell viability assay. Briefly, the cells were cultured in growth medium of DMEM containing 10% heat inactivated FBS supplemented with penicillin (100 U/mL), streptomycin (100 μg/mL) and sodium pyruvate (110 mg/mL). The cells were incubated at 37 °C in 5% $CO_2$ humidified incubator.

**Table 1**
Oligomers used in this study.

| Name | Purpose | Sequence (5′-3′) |
|---|---|---|
| Aj-Prdx6-RTF | qPCR analysis of *AjPrdx6* | CTGCCCGCTGTGTGTTTGTGATT |
| Aj-Prdx6-RTR | qPCR analysis of *AjPrdx6* | GGCCACTCTTTGCTTTGCAGTCA |
| Aj-Prdx6-XpF | ORF amplification (*Eco*RI) | GAGAGAgaattcCCATGCCTGGAATATTGTTAGGAGACG |
| Aj-Prdx6-XpR | ORF amplification (*Hind*III) | GAGAGAaagcttTCATGGCTGGGGTGTGTAGC |
| Aj-EF1α F2 | qPCR for *AjEF1-a* | GAGGTCAAGTCTGTGGAAATGCAC |
| Aj-EF1α R2 | qPCR for *AjEF1-a* | TGATGACCTGAGCAGTGAAGGTAC |

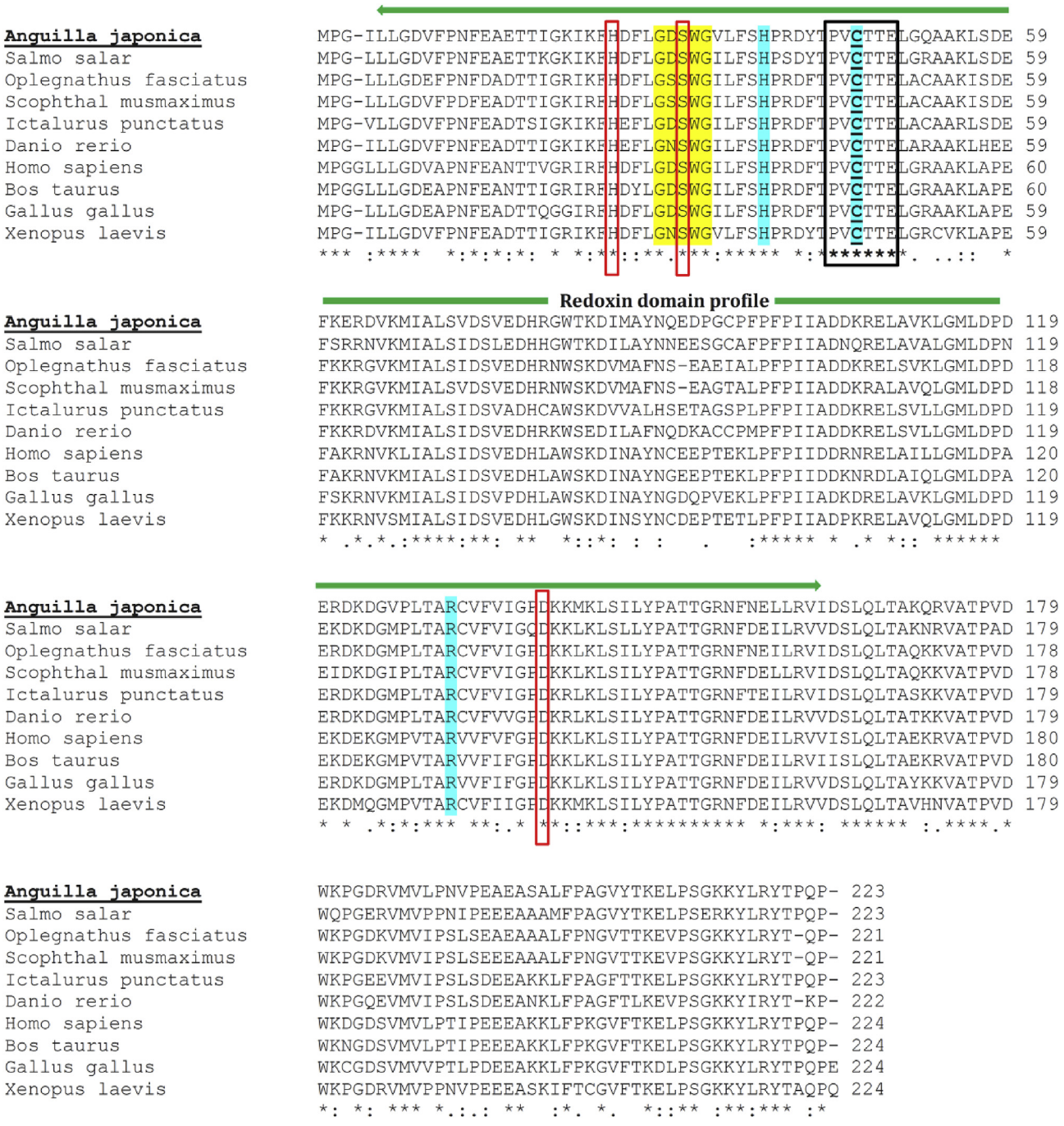


**Fig. 1.** Multiple sequence alignment of different vertebrate Prdx6s. Sequence alignment was performed using ClustalW2 online server. Identical residues in all sequences are indicated by asterisk (*) under the column, conserved substitutions are indicated by colon (:) and semi-conserved substitutions are indicated by dots (.). Deletions are indicated by dashes. The peroxidase catalytic center ($^{44}$PVCTTE$^{49}$) is boxed. Conserved amino acid residues in peroxidase catalytic triad H$^{38}$, C$^{46}$ and R$^{131}$ are highlighted with sky blue color, whereas conserved peroxidatic C$^{46}$ is bolded and underlined. Conserved active site for phospholipase A2 activity ($^{29}$GDSWG$^{33}$) is shaded with yellow. The catalytical triad residues for phospholipase A2 activity (H$^{25}$, S$^{31}$ and D$^{139}$) are indicated by red colored boxes. The accession numbers for Prdx6 homologous are as follows: *Salmo salar*; ACI67008, *Oplegnathus fasciatus*; ADJ21808, *Scophthalmus maximus*; ADJ57694, *Ictalurus punctatus*; NP_001187160, *Danio rerio*; NP_957099, *Gallus gallus*; NP_001034418, *Homo sapiens*; NP_004896, *Bos Taurus*; NP_777068, *Xenopus laevis*; NP_001082669. (For interpretation of the references to colour in this figure legend, the reader is referred to the web version of this article.)

### 2.10. Protective effects of rAjPrdx6 on cultured cells under oxidative stress

In order to investigate the cell-protecting ability of rAjPrdx6 fusion protein under oxidative stress, the cell-viability assay was conducted. Cells were seeded at 2 × $10^5$/mL in 96 well plate and cultured for 24 h. Thereafter, cells were pretreated with different concentrations of rAjPrdx6 fusion protein and 1 mM of dithriothreitol (DTT), and then incubated for 30 min. After the incubation, 500 μM $H_2O_2$ was added and further incubated for 24 h. Experimental treatments are as follows, (1) control cells (2) Cells treated with $H_2O_2$ (500 μM); (3) Cells pre-treated with 100 μg/mL of MBP and 1 mM of DTT followed by 500 μM of $H_2O_2$, (4) Cells pre-treated with 75 μg/mL of rAjPrdx6 and 1 mM of DTT followed by 500 μM of

**Table 2**
Pairwise identity and similarity percentages of AjPrdx6 with selected orthologs at amino acid level.

| Species | Accession no. | Identity (%) | Similarity (%) | Amino acids |
|---|---|---|---|---|
| *Salmo salar* | ACI67008 | 82.5 | 93.3 | 223 |
| *Oplegnathus fasciatus* | ADJ21808 | 81.2 | 92.4 | 221 |
| *Scophthalmus maximus* | ADJ57694 | 81.2 | 91.9 | 223 |
| *Oncorhynchus mykiss* | NP_001158604 | 80.3 | 91.0 | 222 |
| *Ictalurus punctatus* | NP_001187160 | 78.9 | 90.1 | 223 |
| *Danio rerio* | NP_957099 | 77.6 | 91.9 | 222 |
| *Xenopus laevis* | NP_001082669 | 79.5 | 89.3 | 224 |
| *Gallus gallus* | NP_001034418 | 75.9 | 87.1 | 224 |
| *Homo sapiens* | NP_004896 | 75.0 | 87.1 | 224 |
| *Bos taurus* | NP_777068 | 74.6 | 87.1 | 224 |

$H_2O_2$ (5) Cells pre-treated with 100 μg/mL of rAjPrdx6 and 1 mM of DTT followed by 500 μM of $H_2O_2$. Then cell-viability was determined by a standard 3-(4, 5-dimehyl-thiazol-2-yl) 2, 5-diphenyltetrazoium bromide (MTT) assay. During the MTT assay, yellow color tetrazolium bromide is converted into purple colored formazan derivative by mitochondrial succinate dehydrogenase presence in viable cells [42]. After the 24 h incubation period, the MTT solution (50 μL: 2 mg $mL^{-1}$) was added to the each well, to a total reaction volume of 200 μL and incubated for 3 h. Thereafter, supernatants were aspirated and 150 μL of dimethylsulfoxide (DMSO) was added to each well to dissolve the formazan crystals. Then, absorbance was measured by ELISA plate reader at wave length of 540 nm. Relative cell-viability was calculated according to the amount of MTT converted to the insoluble farmazan. The optical density of the formazan generated in the control cells were considered to 100% viability. The data are expressed as mean percentages of the viable cells versus the respective control from triplicate assays.

### 2.11. DNA protecting activity of rAjPrdx6

To determine whether rAjPrdx6 can protect DNA against oxidative stress, the mixed function oxidation (MFO) assay was conducted according to the previous reports with modifications [43,44]. The assay was performed in a total reaction volume of 25 μL with 40 μM of Fe (III), 10 mM of DTT, 10 mM HEPES (pH 7.0) buffer and different concentrations of purified rAjPrdx6 fusion protein. Thereafter, mixtures were incubated at 25 °C for 1 h. Meanwhile, control assays were performed using MBP or column buffer instead of rAjPrdx6 fusion protein. After incubation, 1 μg of pUC19 super coiled DNA was added to each reaction mixture and incubated further at 25 °C for 15 min. Finally reaction mixtures were purified (AccuPrep® PCR Purification Kit, Bioneer, Korea) and analyzed using 1% agarose gel. Triplicated assays were performed to confirm the reliability.

All the qPCR and MTT assay data were subjected to Tukey's method by PASW Statistics 18 software. Values of $p < 0.05$ were considered as statistically significant and all the data are represented as mean standard error (SE).

## 3. Results and discussion

### 3.1. Sequence characterization

The full-length coding sequence of *AjPrdx6* was 669 bp in length (GeneBank accession no: KP246841), which encodes a polypeptide of 223 amino acids with a molecular weight of 24.9 kDa and theoretical isoelectric point of (PI) 5.32. The deduced AjPrdx6 exhibited typical 1-cystine peroxiredoxin family domain architecture, including a redoxin domain profile (residues 35–163) and the N terminus active site ($^{44}$PVCTTE$^{49}$) with active site catalytic cysteine residue (peroxidatic cysteine) ($C^{46}$) (Fig. 1). Furthermore, the catalytical triad residues that involved in peroxidase activity ($H^{38}$, $C^{46}$ and $R^{131}$) and phospholipase A2 activity ($H^{25}$, $S^{31}$ and $D^{139}$) (Fig. 1) were also identified. The signal peptide was not found in AjPrdx6 amino acid sequence by signalP server, suggesting that the AjPrdx6 might be localized in the cytosol. This observation can be validated by a previous report by Wood et al., 2003, which revealed that the mammalian Prdx6 is localized only in cytosolic environments [8].

The EMBOSS needle pairwise sequence alignment showed that the deduced AjPrdx6 amino acid sequence has greatest amino acid identity (82.5%) to that of *Salmo salar*, followed by *Oplegnathus fasciatus* (81.2%), *Scophthalmus maximus* (81.2%), *Oncorhynchus mykiss* (80.3%), *Ictalurus punctatus* (78.9%), *Danio rerio* (77.6%), *Xenopus laevis* (79.5%), *Gallus gallus* (75.9%), *Homo sapiens* (75.0%) and *Bos taurus* (74.6%) (Table 2). According to the report from Manevich et al., 2005, the Prdx6 has more than 95% amino acid and nucleotide similarity among the mammals (Human, pig, rat, mouse and cow) [30]. Likewise, we observed more than 90% amino acid similarity of Prdx6 among the fish species considered herein. The clustalW2 multiple sequence alignment was performed to compare the homology between Prdx6 counterparts from fish, mammals, amphibians and aves (Fig. 1). The redoxin domain profile of AjPrdx6 was highly conserved within all vertebrate Prdx6 counterparts considered. Interestingly, the N-terminus catalytic active site ($^{44}$PVCTTE$^{49}$) including peroxidatic cysteine ($C^{46}$) of AjPrdx6 was completely conserved among all the vertebrate Prdx6 counterparts considered. Moreover, the catalytical triads that involved in peroxidase activity ($H^{38}$, $C^{46}$ and $R^{131}$) and phospholipase A2 activity ($H^{25}$, $S^{31}$ and $D^{139}$) of AjPrdx6 were 100% conserved among selected Prdx6 counterparts from fish, mammalians, aves and amphibians (Fig. 1). Altogether, these observations infer that the AjPrdx6 is indeed a member of Prdx6 subclass and biological activity of AjPrdx6 might be similar to that of known Prdx6s due to the presence of highly conserved active residues.

### 3.2. Phylogenetic analysis

The phylogenetic analysis was carried out to determine the molecular evolutionary relationship of AjPrdx6 with known members of Prdx subclasses from fish, birds, mammals and amphibians using the neighbor joining method (Fig. 2). As expected, three major clades corresponding to typical 2-Cys Prdxs (Prdx1-Prdx4), 1-Cys Prdx (Prdx6) and atypical 2-Cys Prdxs (Prdx5) were observed. Interestingly, the typical 2-Cys Prdx clade was joined to the 1-Cys Prdx clade, while the atypical 2-Cys Prdx class was clustered as a separate branch (Fig. 2). This discrete clustering pattern suggested that the atypical 2-Cys Prdx subclass is distantly related to the typical 2-Cys Prdx and 1-Cys Prdxs. In addition, this observation is a substantial evidence to prove that the closer evolutionary relationship in genetic structure of members of

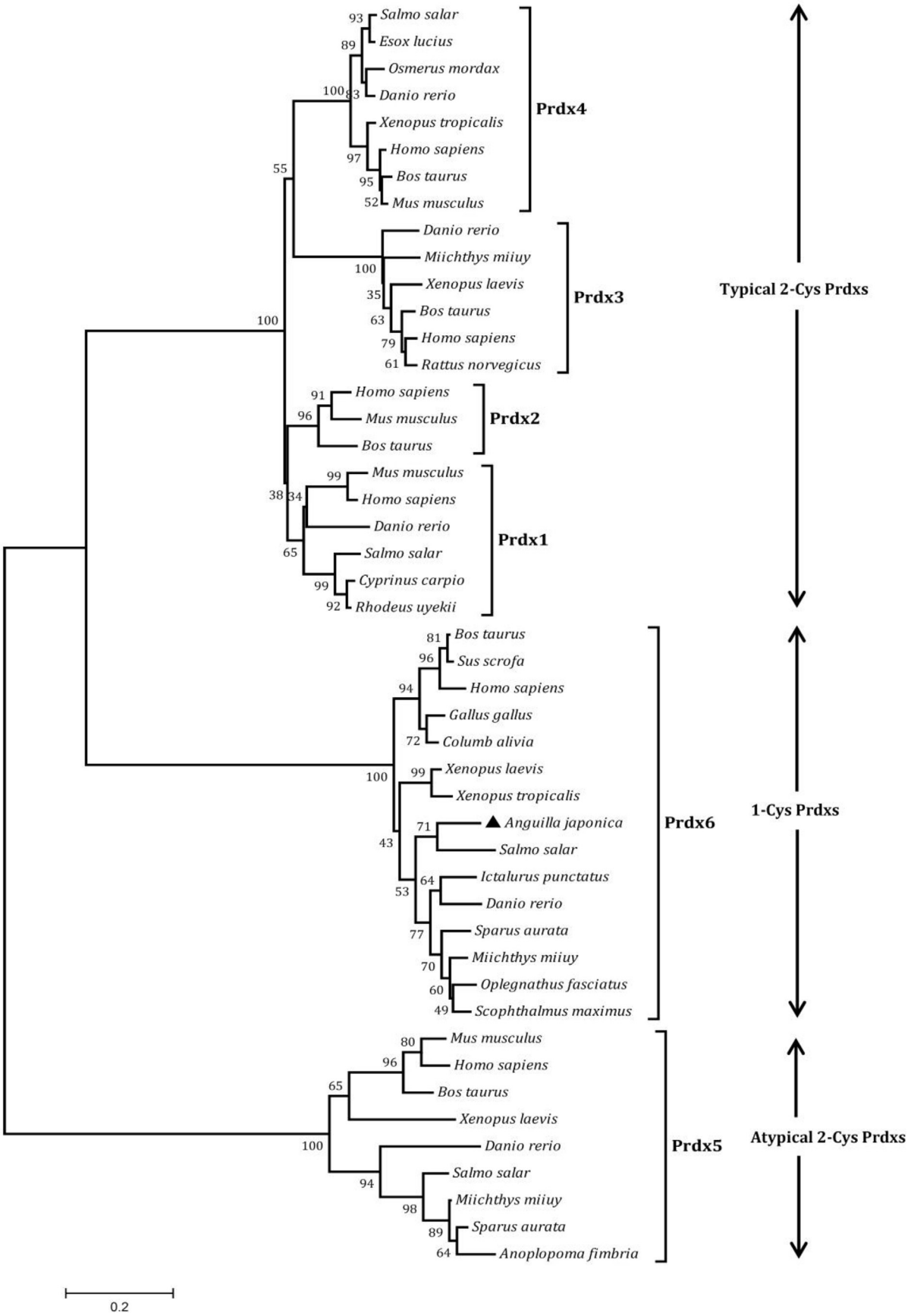
Salmo salar
Esox lucius
Osmerus mordax
Danio rerio
Xenopus tropicalis
Homo sapiens
Bos taurus
Mus musculus
Prdx4
Danio rerio
Miichthys miiuy
Xenopus laevis
Bos taurus
Homo sapiens
Rattus norvegicus
Prdx3
Typical 2-Cys Prdxs
Homo sapiens
Mus musculus
Bos taurus
Prdx2
Mus musculus
Homo sapiens
Danio rerio
Salmo salar
Cyprinus carpio
Rhodeus uyekii
Prdx1
Bos taurus
Sus scrofa
Homo sapiens
Gallus gallus
Columb alivia
Xenopus laevis
Xenopus tropicalis
Anguilla japonica
Salmo salar
Ictalurus punctatus
Danio rerio
Sparus aurata
Miichthys miiuy
Oplegnathus fasciatus
Scophthalmus maximus
Prdx6
1-Cys Prdxs
Mus musculus
Homo sapiens
Bos taurus
Xenopus laevis
Danio rerio
Salmo salar
Miichthys miiuy
Sparus aurata
Anoplopoma fimbria
Prdx5
Atypical 2-Cys Prdxs
0.2

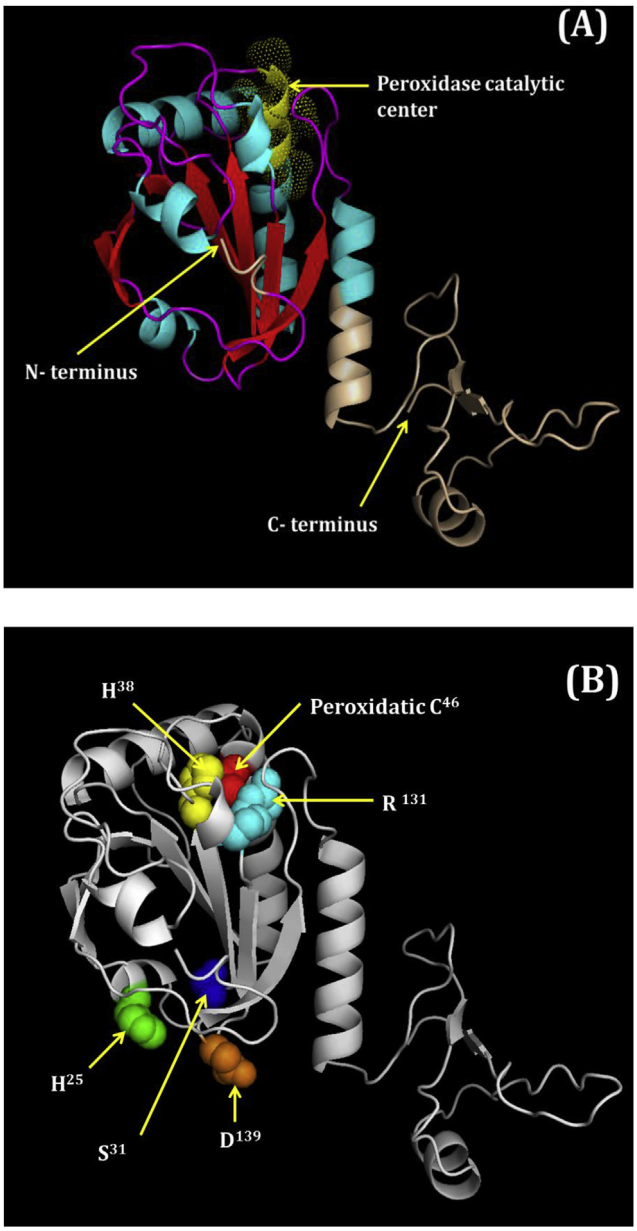


**Fig. 3.** (A) Computer simulation model generated for the AjPrdx6. Tertiary structure elements belonging to the redoxin domain profile: (sky blue) α-helixes, (Red) β-sheets. The peroxidase catalytic center is represented with yellow dots. (B) 3D structure of AjPrdx6 with important conserved amino acid residues. The Peroxidatic $C^{46}$ is marked with red color sphere, whereas rest of the amino acid residues in catalitical triad for peroxidase activity are marked with yellow ($H^{38}$) and sky blue ($R^{131}$) spheres. The corresponding conserved amino acid residues for phospholipase A2 catalytic triad are denoted by green ($H^{25}$), blue ($S^{31}$) and orange ($D^{139}$) spheres. (For interpretation of the references to colour in this figure legend, the reader is referred to the web version of this article.)

typical 2-Cys Prdx subclass (Prdx1, Prdx2, Prdx3 and Prdx4) [45]. As depicted in Fig. 2, the AjPrdx6 was positioned in the piscine subgroup of 1-Cys Prdx clade exhibiting a highest evolutionary proximity to *S. salar* Prdx6. Moreover, Prdx6 counterparts from mammals, avians and amphibians were separately clustered in their corresponding sub-clades in the 1-Cys Prdx clade. Altogether, our phylogenetic study revealed that AjPrdx6 shares homology to known Prdx6 counterparts.

### 3.3. Predicted 3D homology modal of AjPrdx6

The 3D structural modal of AjPrdx6 protein was generated by I-TASSER online server [46] using top ten compatible templates from the Research Collaboratory for Structural Bioinformatics (RCSB) protein data bank. All the obtained templates exhibited higher identity (67%–75%) to the query sequence, as well as normalized Z-score of the treading alignment was more than one. Those observations confidently proved that the reliability of predicted modal of AjPrdx6. Moreover, the generated modal of AjPrdx6 showed 0.94 ± 0.05 of estimated TM score and 1.62 of confidence score (C-Score), suggesting that its closer similarity to the native structure of known Prdx6 [46]. The tertiary structure of AjPrdx6 was composed of nine core stranded β-sheets flanked by seven α-helixes (Fig. 3A). The C-terminus, N-terminus and redoxin domain profile were identified in the generated modal of AjPrdx6 (Fig. 3A). Furthermore, the active site peroxidatic cysteine residue ($C^{46}$), catalytic triads that involved in peroxidase activity ($H^{38}$, $C^{46}$ and $R^{131}$) and phospholipase A2 activity ($H^{25}$, $S^{31}$ and $D^{139}$) were identified (Fig. 3B). Crystal structural analysis of human Prdx6 identified $C^{47}$, $H^{39}$ and $R^{132}$ as catalytic triad for peroxidase activity; among which the peroxidatic $C^{47}$ form a hydrogen bond with $H^{39}$ in peroxidase catalytic triad and $R^{132}$ is involved in electrostatic activation of $C^{47}$ [30,47,48]. According to the generated modal of AjPrdx6, corresponding amino acid residues for peroxidase catalytical triad of AjPrdx6 ($H^{38}$, $C^{46}$ and $R^{131}$) were positioned in the same plane and adjacent to each other (Fig. 3B). In human, the Prdx6 also contains a catalytic triad for phospholipase A2 activity ($H^{26}$, $S^{32}$ and $D^{140}$) [30]. Crystal structural analysis of human Prdx6 demonstrated that the catalytic $C^{47}$ was positioned at 25 Å away from the phospholipase A2 catalytic center ($S^{32}$), thereby prohibits the interaction of two active centers for different activities [30]. Likewise, we observed the two catalytic active centers that responsible for peroxidase activity ($C^{46}$) and phospholipase A2 activity ($S^{31}$) at two significantly different positions in the generated modal of AjPrdx6 (Fig. 3B). Collectively these finding demonstrated that the 3D arrangement of AjPrdx6 is compatible with its human ortholog.

### 3.4. Tissue distribution analysis of AjPrdx6

Tissue specific distribution of *AjPrdx6* mRNA transcripts in unchallenged Japanese eels were determined by qPCR analysis using *AjEF1-a* as an internal control. Expression fold of *AjPrdx6* in each tissue was calculated relative to spleen. The *AjPrdx6* was ubiquitously expressed in all the immune and non-immune tissues examined, including liver, spleen, brain, muscle, heart, skin, kidney,

**Fig. 2.** Phylogenetic tree of known Prdxs from different species including the AjPrdx6. The tree was constructed using neighbor-joining method. Bootstrap values are shown next to the branches based on 1000 replications. The accession numbers for Prdx homologous are as follows: Prdx1 (*Mus musculus*; NP_035164, *Homo sapiens*; NP_002565, *Danio rerio*; NP_001013489, *Salmo salar*; NP_001134295, *Cyprinus carpio*; ABC59223, *Rhodeus uyekii*; AGU16435); Prdx2 (*Homo sapiens*; AAH39428, *Mus musculus*; NP_035693, *Bos Taurus*; AAG53659); Prdx3 (*Danio rerio*; AAH92846, *Miichthys miiuy*; AGT56738, *Xenopus laevis*; AEM44540, *Bos taurus*; AAI03010, *Homo sapiens*; AAH08435, *Rattus norvegicus*; EDL94585); Prdx4 (*Salmo salar*; ACI69656, *Esox Lucius*; ACO14427, *Osmerus mordax*; ACO09915, *Danio rerio*; NP_001082894, *Xenopus (Silurana) tropicalis*; NM_001006811, *Homo sapiens*; EAW98996, *Bos Taurus*; NM_174433, *Mus musculus*; NM_016764); Prdx5 (*Mus musculus*; AAH08174, *Homo sapiens*; AAI13724, *Bos Taurus*; NM_174749, *Xenopus laevis*; AEM44542, *Danio rerio*; NP_001019577, *Salmo salar*; ACI66176, *Miichthys miiuy*; AGT56736, *Sparus aurata*; G0T336, *Anoplopoma fimbria*; C3KHS6); Prdx6 (*Bos Taurus*; NP_777068, *Sus scrofa*; NP_999573, *Homo sapiens*; NP_004896, *Gallus gallus*; NP_001034418, *Columba livia*; NP_001269769, *Xenopus laevis*; NP_001082669, *Xenopus (Silurana) tropicalis*; NP_989102, *Salmo salar*; ACI67008, *Ictalurus punctatus*; NP_001187160, *Danio rerio*; NP_957099, *Sparus aurata*; ADI78069, *Miichthys miiuy*; AGK83638, *Oplegnathus fasciatus*; ADJ21808, *Scophthalmus maximus*; ADJ57694).

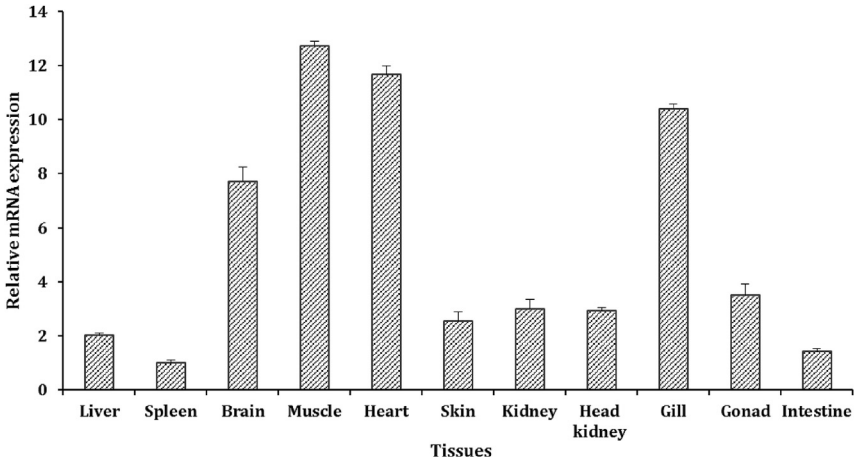


**Fig. 4.** Tissue specific expression analysis of *AjPrdx6* mRNA in healthy *Anguilla japonica* by qPCR. The mRNA expression level of each tissue is expressed relative to the mRNA expression in spleen tissue. Each bar represents the standard error (SE) of five replicates (n = 5).

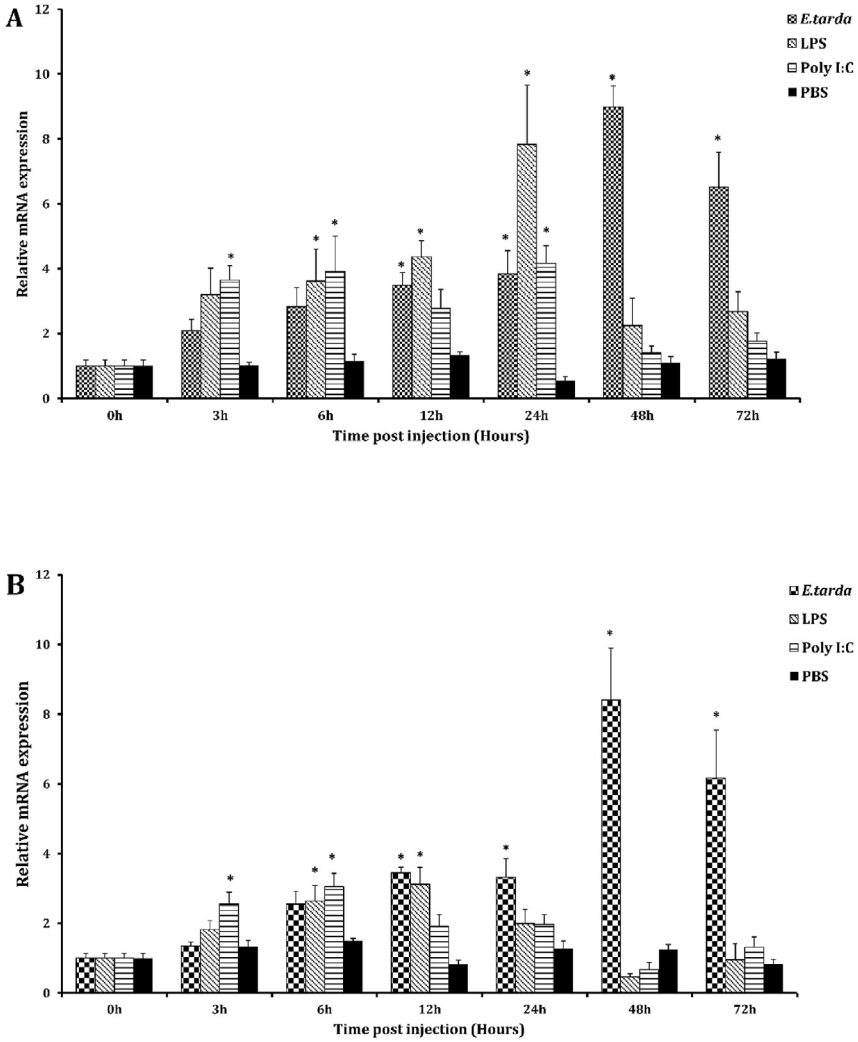


**Fig. 5.** Relative mRNA expression pattern of *AjPrdx6* after the stimulation with *Edwardsiella tarda*, LPS and Poly I:C in liver (A) and spleen (B). The expression analysis of *AjPrx6* was determined by qPCR. Livak $2^{-\Delta\Delta CT}$ method was used to calculate relative expression levels of *AjPrdx6* using *Anguilla japonica EF-1a* as an internal control gene. Each bar represents the standard error (SE) of five individual samples (n = 5). Asterisk (*) represents the significant difference in expression against the un-injected control ($P < 0.05$).

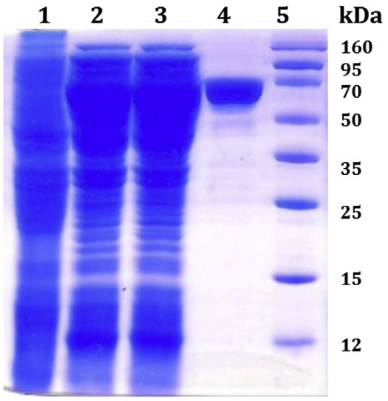


**Fig. 6.** SDS-PAGE analysis of the rAjPrdx6 fusion protein in *E. coli* BL21. Lane 1, total protein of un-induced *E. coli* (BL21); lane 2, total cellular extract from *E. coli* BL21 after IPTG induction; lane 3, soluble fraction of cellular extract after IPTG induction; lane 4, purified recombinant fusion protein (rAjPrdx6) after IPTG induction; Lane 5, molecular weight marker.

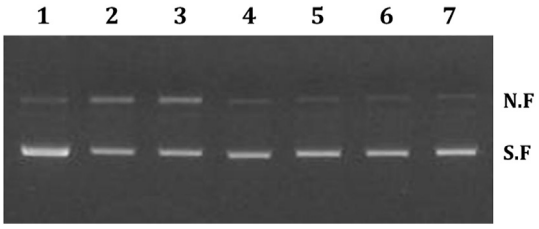


**Fig. 8.** Recombinant AjPrdx6 mediated inactivation of supercoiled DNA cleavage by mixed function oxidation assay. (1) pUC19 (1 μg) plasmid DNA without incubation; (2) Column buffer + 40 μM of Fe (III) + 10 of mM DTT + 10 mM of HEPS + 1 μg of pUC19; (3) MBP (10 μg) + 40 μM of Fe (III) + 10 of mM DTT + 10 mM of HEPS + 1 μg of pUC19; (4) rAjPrdx6 (2.5 μg) + 40 μM of Fe (III) + 10 of mM DTT + 10 mM of HEPS + 1 μg of pUC19; (5) rAjPrdx6 (5 μg) + 40 μM of Fe (III) + 10 of mM DTT + 10 mM of HEPS + 1 μg of pUC19; (6) rAjPrdx6 (10 μg) + 40 μM of Fe (III) + 10 of mM DTT + 10 mM of HEPS + 1 μg of pUC19; (7) Column buffer + 10 mM of HEPS + 1 μg of pUC19, N.F: nicked form, S.F: super coiled form.

head kidney, gill, gonad and intestine. As shown in Fig. 4, *AjPrdx6* mRNA was highly expressed in muscle followed by heart, gill and brain, while lowest expression fold was detected in spleen. Number of studies have demonstrated that *Prdx6* mRNA constitutively expressed in all major organs of mammals with the prominent expression levels in lungs [30–32,49]. Expression analysis of *Prdx6* in fish showed its ubiquitous distribution among the tissues tested. Wen-jiang Zheng and group revealed that *Prdx6* was highly expressed in blood, heart and muscle among the tested tissues of turbot (*Scophthalmus maximus*), lowest level was detected in spleen [24]. Expression of rock bream (*Oplegnathus fasciatus*) *Prdx6* was predominantly detected in liver followed by intestine, while lowest in spleen, skin and gill [25]. In gilthead sea bream (*Sparus aurata*), Prdx6 was expressed in all tested tissues with highest expression level in liver [11]. Liping Ren and group reported that miiuy croaker (*Miichthys miiuy*) peroxiredoxin 5 was prominently expressed in muscles, and they proposed this observation might be due to the antioxidant function of peroxiredoxin 5 to eliminate $H_2O_2$ and other harmful free radicals produced by the muscles during the energy production process, since muscles are considered as one of the fundamental energy producing tissue in the body [50]. Moreover W.j.Zheng et al. (2010) described that *Prdx6* was involved in cellular maintenance under normal physiological conditions in muscles of *Scophthalmus maximus* [24]. In this study muscle tissue showed the highest expression level of *Prdx6* in Japanese eel. Hence

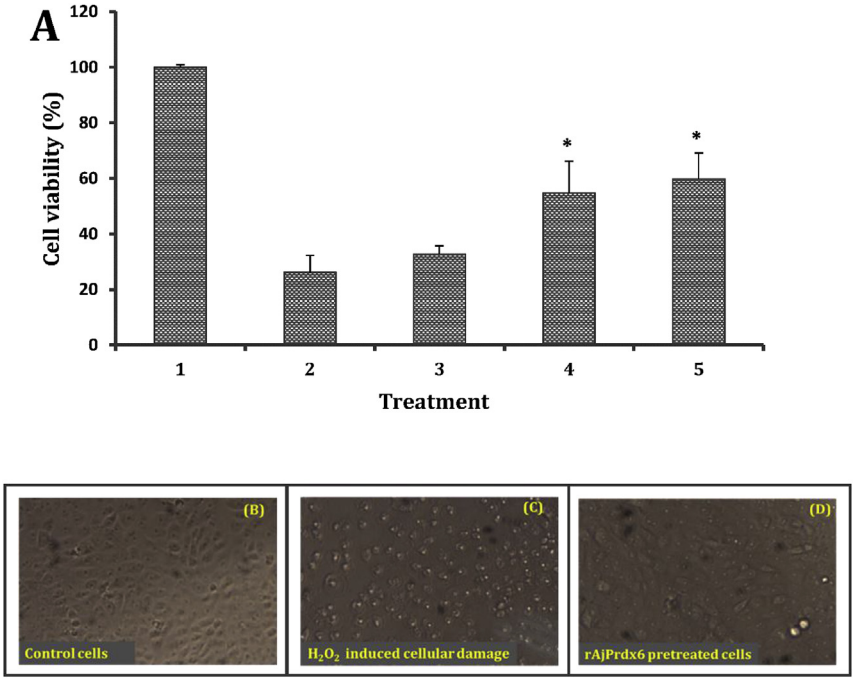


**Fig. 7.** (A) Effects of rAjPrdx6 on cell growth and viability in 500 μM $H_2O_2$ exposed to vero cells. Cells were seeded at $2 \times 10^5$/mL and pretreated with the different concentration combinations of rAjPrdx6 for 30 min followed by treatment with 500 μM $H_2O_2$ for 24 h. Cell viability was determined by MTT assay. Treatments: (1) control cells; (2) cells treated with $H_2O_2$ (500 μM), (3) cells pretreated with MBP (100 μg/mL) and DTT (1 mM) followed by $H_2O_2$ (500 μM); (4) cells pretreated with 75 μg/mL of rAjPrdx6 and 1 mM of DTT followed by 500 μM of $H_2O_2$ (5) cells pretreated with 100 μg/mL of rAjPrdx6 and 1 mM of DTT followed by 500 μM of $H_2O_2$. Each bar represents the standard error (SE) of three individual samples (n = 3). Asterisk (*) represents the significant difference in percentage of cell viability against the rAjPrdx6 untreated sample (Treatment 2) ($P < 0.05$). (B) Light microscopic image of control vero cells. (C) Light microscopic image of vero cells treated with $H_2O_2$ (500 μM). (D) Microscopic image of vero cells treated with 100 μg/mL of rAjPrdx6 and 1 mM of DTT followed by 500 μM of $H_2O_2$.

we suggested it could be due to the high potential of muscles to express *Prdx6* to eliminate $H_2O_2$ and other toxic free radicals during the energy producing process in Japanese eel.

### 3.5. Expression profile of AjPrdx6 upon E. tarda, LPS and poly I:C challenge

In order to determine the innate immune responses of *AjPrdx6* upon different stimuli, naïve Japanese eels were challenged with Gram negative fish pathogen *E. tarda*, LPS and poly I:C. Thereafter, the relative mRNA expression profiles of *AjPrdx6* in liver and spleen were determined by qPCR using *AjEF1-a* as an internal control gene. The liver and spleen are believed to play pivotal role in early innate immune responses against pathogenic infections in vertebrates, and several researchers have targeted those tissues to determine the temporal mRNA expression profiles of innate immunity-related genes. Only one peak for both *AjPrdx6* and *AjEF1-a* was detected at corresponding melting temperature in the dissociation curve analysis, suggesting that the target was specifically amplified. As shown in Fig. 5A the mRNA transcripts of *AjPrdx6* were gradually upregulated until 48 h p.i. of *E. tarda* with significant ($P < 0.05$) inductions at 12 h, 24 h, 48 h and 72 h p.i. After the LPS stimulation, gradual upregulation of *AjPrdx6* transcripts were detected at early to middle phase, at 6 h–24 h (Fig. 5A). Moreover, the basal mRNA transcript level of *AjPrdx6* was significantly elevated at 3 h, 6 h and 24 h p.i. upon the poly I:C injection (Fig. 5A).

As depicted in Fig. 5B, after the injection of *E. tarda* the *AjPrdx6* mRNA transcripts were upregulated throughout the experiment at 12 h–72 h p.i. in spleen tissue. However, the *AjPrdx6* mRNA transcripts were gradually upregulated until 12 h p.i. with the significant inductions at 6 h and 12 h after the LPS injection (Fig. 5B). Nevertheless, *AjPrdx6* transcripts were down-regulated at 48 h and 72 h p.i. after the LPS injection in spleen tissues (Fig. 5B). In spleen, poly I:C injection engendered significant up-regulation of *AjPrdx6* mRNA transcripts at 3 h and 6 h p.i., while the expression fold was down-regulated at 48 h p.i. (Fig. 5B).

Several previous studies have demonstrated that *Prdx6* transcription is up-regulated under various pathological conditions in many organisms including teleost. Wen-jiang Zheng and group demonstrated that *Prdx6* mRNA expression is upregulated upon *Listonella anguillarum* and poly I:C injections in the spleen and liver tissues of *Scophthalmus maximus* [24]. Furthermore, it has been shown that *Prdx6* transcription in liver tissues of *O. faciatus* is up-regulated after the poly I:C injection [25]. Nevertheless, down-regulations of *Prdx6* in gill tissues of disk abalone against viral infection [27] and haemocytes in *Eriocheir sinensis* (chinese mitten crab) upon *L. anguillarum* injection have also been reported [26]. Moreover numerous studies have demonstrated that expression of *Prdx6* could be modulated in several organisms due to different stress conditions, like thermal exposure [34] and environmental pollutants [28].

In this study, almost similar expression profiles of *AjPrdx6* mRNA were observed in liver and spleen tissues upon *E. tarda* injection (Fig. 5). *E. tarda* is a potent Gram negative fish pathogen [51] which could be detected by pathogen recognition receptors through PAMPs. The LPS, a pivotal PAMP in Gram negative bacteria, can induce potent immune response in host after being recognized by toll like receptor 4 (TLR4). Thereafter, phagocytes and macrophages are activated to induce the production of ROS and thereby counterattack the pathogenic invasion [52,53]. In order to scavenge the excess ROS or maintain the cellular oxidative balance under the pathological condition, transcription of peroxidases should be modulated accordingly. Previous studies revealed that up-regulation of *Prdx6* in liver cells of mouse under $H_2O_2$ stress [54]. Moreover, Dong Yang and group found that *Prdx6* knockout mice were susceptible for acute oxidative stress after LPS-challenge, thereby induce the lung injury compared to the wild type mice [55]. Based on these facts, we suggest that up-regulation of *AjPrdx6* mRNA transcripts might be due to the detection of PAMPs in *E. tarda* by PRRs in phagocytes or macrophages in liver and spleen. The lower induction fold of *AjPrdx6* mRNA transcripts at 3 h–24 h p.i. could be plausibly attributed to the fact of immune evasion mechanism elicited by pathogen to overcome host immune response. According to the phenomena of pathogen evasion, bacteria like *E. tarda* can reduce intracellular ROS production in host [56]. Therefore, expression of antioxidant enzymes including *Prdx6* may be suppressed at early phase of *E. tarda*-injection. However, host cells aroused marked immune responses to counterattack the bacterial invasion with the time; thereby *AjPrdx6* mRNA transcripts were highly up-regulated at latter phase of experiment upon *E. tarda* injection in liver and spleen. Interestingly, after LPS injection, the *AjPrdx6* mRNA transcripts were also up-regulated in the liver (3 h–72 h p.i.) and spleen (3 h–24 h p.i.) (Fig. 5A and B), whereby proved our previous suggestions.

The expression profile of *AjPrdx6* in liver upon poly I:C injection was quite similar to that of spleen. Poly I:C is a double stranded RNA mimic which is sensed by TLR3 and ultimately induce production of type 1 interferons (IFNs) and proinflammatory cytokines [57]. Previous reports documented that RNA virus could enhance the production of ROS after infection, thereby the antioxidant system is activated to protect the host form oxidative damage [58]. This hypothesis is in accordance with the fact that up-regulation of *AjPrdx6* mRNA transcripts upon poly I:C injection in spleen and liver.

### 3.6. Over expression and purification of rAjPrdx6

In order to characterize the antioxidant properties of AjPrdx6, the coding sequence was cloned into the pMAL-c2X expression vector and expressed as a fusion protein with MBP (Fig. 6). SDS-PAGE resolved a single purified protein band, confirming successful purification of the fusion protein and indicating a molecular mass of ~67 kDa. The size of the band was consistent with the predicted molecular mass of AjPrdx6 (24.9 kDa), since the molecular mass of MBP is ~42.5 kDa.

### 3.7. Protective effects of rAjPrdx6 on cultured cells under oxidative stress

The cytotoxic effect of $H_2O_2$ on vero cells in the presence of purified rAjPrdx6 fusion protein with different concentrations was determined by the MTT assay. The Prdxs are considered as a thiol dependent enzymes, which required the action of the electron donors like thioredoxin, glutaredoxin, cyclophilin or glutathione for complete their catalytic cycle [59]. Therefore, DTT was used as an electron donor for this experiment. According to the results, up to 50% cell survival was observed in rAjPrdx6 fusion protein treated cell samples (with 75 and 100 μg/mL rAjPrdx6) under the $H_2O_2$ induced oxidative stress (Fig. 7A). The MBP treated cells did not show significant cell viability compared to the rAjPrdx6 un-treated cells, suggesting that its activity was negligible on cell viability (Fig. 7A, Treatment 3). Moreover, microscopic images revealed that cells were severely damaged after $H_2O_2$ treatment (Fig. 7C), while rAjPrdx6 pretreated cells were able to survive under oxidative stress (Fig. 7D). Cell-protecting ability of the Prdx6 under oxidative stress has been proved by previous experiments, for example, C. Nikapitiya et al., 2009 and W. j. Zheng et al., 2010 described that $H_2O_2$ scavenging ability of recombinant Prdx6 from disk abalone and turbot, respectively [24,27]. Moreover, Prdx6 overexpressing keratinocytes isolated from transgenic mice showed significant resistant to the cytotoxicity generated by ROS like $H_2O_2$ [60]. Some

previous evidences demonstrated that enhanced protecting activity of 1-Cys Prdx overexpressing cells against peroxide mediated cell membrane damage [61]. As the suggestion of Kumin. et al. (2006), the protecting effects of Prdx6 were elicited by its peroxidase activity, since Prdx6 is considered as bifunctional enzyme [60]. Development of effective antioxidant enzymes is needed for protection of the organism from pathogenesis aroused by oxidative stress mediated cell damage. During the pathogical conditions associated with enhanced level of ROS, the expression of Prdx6 was strongly elevated in the affected tissues to overcome severity of the pathogenesis [60]; hence protect the cells and tissues from ROS mediated oxidative damage. Interestingly, our observations complied with these previous evidences suggesting the potency of rAjPrdx6 on cell protection under $H_2O_2$ mediated oxidative stress by reducing harmful $H_2O_2$ into nontoxic products. Furthermore, the AjPrdx6 might be expressed as an active antioxidant enzyme to overcome the pathogenesis elicited by the ROS mediated cellular damage in Japanese eel.

### 3.8. Invitro DNA protecting activity of rAjPrdx6 against oxidative damage

DNA protecting activity of rAjPrdx6 in oxidative damage was determined using MFO assay [62]. The MFO system can generate ROS [63] including superoxides, hydroxyl radicals and hydrogen peroxides by metal catalyzed Fenton reactions [64]. Therefore, presence of the MFO system can induce the nicking of supercoiled plasmid DNA into open circular form and leads to the sever DNA damage [62,64]. In this study, we assayed inhibition of the conversion of supercoiled pUC19 plasmid DNA into open circular or nicked forms by rAjPrdx6. As depicted in Fig. 8, high percentage of supercoiled pUC19 plasmid DNA was converted into the nicked form after the treatment with complete MFO system when rAjPrdx6 was absent (Fig. 8, Treatment: 2) compared to the control treatment (Treatment 7). However, in the presence of rAjPrdx6 (2.5 μg, 5 μg and 10 μg) nicking of supercoiled pUC19 plasmid DNA into open circular form was significantly inhibited (Fig. 8, Treatments 4, 5, 6). Moreover, intensity of the bands corresponding to nicked conformation of pUC19 plasmid DNA was slightly reduced with the increasing amount of rAjPrdx6 (Fig. 8, Treatments 4, 5, 6). MBP treatment did not show any significant reduction of intensity of the band corresponding to supercoiled DNA, suggesting that MBP was not actively involved in DNA protection against metal catalyzed DNA damage (Fig. 8, treatment 3). According to the assay results, we can assume that the rAjPrdx6 effectively scavenged ROS generated *via* metal catalyzed Fenton type reaction, thereby protect the DNA from oxidative damage. Moreover, previous experiments have demonstrated that the DNA protecting ability of recombinant Prdx6 from eukaryotes under oxidative-damaging conditions [25,27]. Therefore, based on our observations, together with previous experimental results, we suggest the AjPrdx6 may play a pivotal role as an active antioxidant enzyme to eliminate harmful ROS in Japanese eel under oxidative stress.

## 4. Conclusion

In conclusion, Peroxiredoxin 6 from Japanese eel (AjPrdx6) was identified and molecularly characterized at transcriptional and protein levels. The findings of this study demonstrate that the AjPrdx6 was indeed a member of 1- Cysteine peroxiredoxin subfamily. Ubiquitous expression of *AjPrdx6* mRNA transcripts was detected in all the tissues of unchallenged eels. Moreover, expression of *AjPrdx6* mRNA transcripts in liver and spleen were significantly up-regulated by live-bacterial pathogen and PAMPs. Furthermore, cultured vero cells were significantly protected by rAjPrdx6 protein against oxidative stress. Additionally, we provided an evidence for its DNA protecting activity. Collectively, our findings suggest that AjPrdx6 play a pivotal role in defense of cellular oxidative stress and host immune responses against pathological conditions.

## Acknowledgment

This research was a part of the project titled ' Fish Vaccine Research Center', funded by the Ministry of Oceans and Fisheries, Republic of Korea and supported by a grant from the National Fisheries Research and development Institute (NFRDI, RP-2015-AQ-0003), Republic of Korea.

## References

[1] H. Kamata, H. Hirata, Redox regulation of cellular signalling, Cell. Signal. 11 (1999) 1–14.
[2] V.J. Thannickal, B.L. Fanburg, Reactive oxygen species in cell signaling, Am. J. Physiol. Lung Cell. Mol. Physiol. 279 (2000) L1005–L1028.
[3] J. Nordberg, E.S. Arner, Reactive oxygen species, antioxidants, and the mammalian thioredoxin system, Free Radic. Biol. Med. 31 (2001) 1287–1312.
[4] E.R. Stadtman, R.L. Levine, Protein oxidation, Ann. N. Y. Acad. Sci. 899 (2000) 191–208.
[5] S. Yla-Herttuala, Oxidized LDL and atherogenesis, Ann. N. Y. Acad. Sci. 874 (1999) 134–137.
[6] E. Cadenas, K.J. Davies, Mitochondrial free radical generation, oxidative stress, and aging, Free Radic. Biol. Med. 29 (2000) 222–230.
[7] S. Kawazu, K. Komaki-Yasuda, H. Oku, S. Kano, Peroxiredoxins in malaria parasites: parasitologic aspects, Parasitol. Int. 57 (2008) 1–7.
[8] Z.A. Wood, E. Schroder, J. Robin Harris, L.B. Poole, Structure, mechanism and regulation of peroxiredoxins, Trends Biochem. Sci. 28 (2003) 32–40.
[9] S.G. Rhee, H.Z. Chae, K. Kim, Peroxiredoxins: a historical overview and speculative preview of novel mechanisms and emerging concepts in cell signaling, Free Radic. Biol. Med. 38 (2005) 1543–1552.
[10] M.E. Perez-Perez, A. Mata-Cabana, A.M. Sanchez-Riego, M. Lindahl, F.J. Florencio, A comprehensive analysis of the peroxiredoxin reduction system in the Cyanobacterium Synechocystis sp. strain PCC 6803 reveals that all five peroxiredoxins are thioredoxin dependent, J. Bacteriol. 191 (2009) 7477–7489.
[11] J. Perez-Sanchez, A. Bermejo-Nogales, J.A. Calduch-Giner, S. Kaushik, A. Sitja-Bobadilla, Molecular characterization and expression analysis of six peroxiredoxin paralogous genes in gilthead sea bream (Sparus aurata): insights from fish exposed to dietary, pathogen and confinement stressors, Fish Shellfish Immunol. 31 (2011) 294–302.
[12] H.Z. Chae, S.W. Kang, S.G. Rhee, Isoforms of mammalian peroxiredoxin that reduce peroxides in presence of thioredoxin, Methods Enzym. 300 (1999) 219–226.
[13] H.R. Ellis, L.B. Poole, Novel application of 7-chloro-4-nitrobenzo-2-oxa-1,3-diazole to identify cysteine sulfenic acid in the AhpC component of alkyl hydroperoxide reductase, Biochemistry 36 (1997) 15013–15018.
[14] H.R. Ellis, L.B. Poole, Roles for the two cysteine residues of AhpC in catalysis of peroxide reduction by alkyl hydroperoxide reductase from Salmonella typhimurium, Biochemistry 36 (1997) 13349–13356.
[15] M. Aran, D.S. Ferrero, E. Pagano, R.A. Wolosiuk, Typical 2-Cys peroxiredoxins–modulation by covalent transformations and noncovalent interactions, FEBS J. 276 (2009) 2478–2493.
[16] S.Y. Kim, E. Chun, K.Y. Lee, Phospholipase A(2) of peroxiredoxin 6 has a critical role in tumor necrosis factor-induced apoptosis, Cell Death Differ. 18 (2011) 1573–1583.
[17] A.B. Fisher, Peroxiredoxin 6: a bifunctional enzyme with glutathione peroxidase and phospholipase A(2) activities, Antioxidants Redox Signal. 15 (2011) 831–844.
[18] A. Mitsumoto, Y. Takanezawa, K. Okawa, A. Iwamatsu, Y. Nakagawa, Variants of peroxiredoxins expression in response to hydroperoxide stress, Free Radic. Biol. Med. 30 (2001) 625–635.
[19] J.W. Chen, C. Dodia, S.I. Feinstein, M.K. Jain, A.B. Fisher, 1-Cys peroxiredoxin, a bifunctional enzyme with glutathione peroxidase and phospholipase A2 activities, J. Biol. Chem. 275 (2000) 28421–28427.
[20] E.F. Domino, A.E. Wilson, Brain acetylcholine in morphine pellet implanted rats given naloxone, Psychopharmacologia 41 (1975) 19–22.
[21] H.M. Yun, K.R. Park, H.P. Lee, D.H. Lee, M. Jo, D.H. Shin, et al., PRDX6 promotes lung tumor progression via its GPx and iPLA2 activities, Free Radic. Biol. Med. 69 (2014) 367–376.
[22] Y. Wang, Y. Manevich, S.I. Feinstein, A.B. Fisher, Adenovirus-mediated transfer of the 1-cys peroxiredoxin gene to mouse lung protects against hyperoxic injury, Am. J. Physiol. Lung Cell Mol. Physiol. 286 (2004) L1188–L1193.
[23] A.K. Singh, H. Shichi, A novel glutathione peroxidase in bovine eye. Sequence analysis, mRNA level, and translation, J. Biol. Chem. 273 (1998) 26171–26178.
[24] W.J. Zheng, Y.H. Hu, M. Zhang, L. Sun, Analysis of the expression and

antioxidative property of a peroxiredoxin 6 from Scophthalmus maximus, Fish Shellfish Immunol. 29 (2010) 305–311.
[25] M. De Zoysa, J.H. Ryu, H.C. Chung, C.H. Kim, C. Nikapitiya, C. Oh, et al., Molecular characterization, immune responses and DNA protection activity of rock bream (Oplegnathus fasciatus), peroxiredoxin 6 (Prx6), Fish Shellfish Immunol. 33 (2012) 28–35.
[26] C. Mu, J. Zhao, L. Wang, L. Song, H. Zhang, C. Li, et al., Molecular cloning and characterization of peroxiredoxin 6 from Chinese mitten crab Eriocheir sinensis, Fish Shellfish Immunol. 26 (2009) 821–827.
[27] C. Nikapitiya, M. De Zoysa, I. Whang, C.G. Kim, Y.H. Lee, S.J. Kim, et al., Molecular cloning, characterization and expression analysis of peroxiredoxin 6 from disk abalone Haliotis discus discus and the antioxidant activity of its recombinant protein, Fish Shellfish Immunol. 27 (2009) 239–249.
[28] E. David, A. Tanguy, D. Moraga, Peroxiredoxin 6 gene: a new physiological and genetic indicator of multiple environmental stress response in Pacific oyster Crassostrea gigas, Aquat. Toxicol. 84 (2007) 389–398.
[29] S.W. Kang, I.C. Baines, S.G. Rhee, Characterization of a mammalian peroxiredoxin that contains one conserved cysteine, J. Biol. Chem. 273 (1998) 6303–6311.
[30] Y. Manevich, A.B. Fisher, Peroxiredoxin 6, a 1-Cys peroxiredoxin, functions in antioxidant defense and lung phospholipid metabolism, Free Radic. Biol. Med. 38 (2005) 1422–1432.
[31] Y. Mo, S.I. Feinstein, Y. Manevich, Q. Zhang, L. Lu, Y.S. Ho, et al., 1-Cys peroxiredoxin knock-out mice express mRNA but not protein for a highly related intronless gene, FEBS Lett. 555 (2003) 192–198.
[32] G. Leyens, I. Donnay, B. Knoops, Cloning of bovine peroxiredoxins-gene expression in bovine tissues and amino acid sequence comparison with rat, mouse and primate peroxiredoxins, Comp. Biochem. Physiol. B Biochem. Mol. Biol. 136 (2003) 943–955.
[33] Q. Wang, K. Chen, Q. Yao, Y. Zhao, Y. Li, H. Shen, et al., Identification and characterization of a novel 1-Cys peroxiredoxin from silkworm, Bombyx mori, Comp. Biochem. Physiol. B Biochem. Mol. Biol. 149 (2008) 176–182.
[34] H. Park, I.Y. Ahn, H. Kim, J. Cheon, M. Kim, Analysis of ESTs and expression of two peroxiredoxins in the thermally stressed Antarctic bivalve Laternula elliptica, Fish Shellfish Immunol. 25 (2008) 550–559.
[35] H.S. Kim, Y. Manevich, S.I. Feinstein, J.H. Pak, Y.S. Ho, A.B. Fisher, Induction of 1-cys peroxiredoxin expression by oxidative stress in lung epithelial cells, Am. J. Physiol. Lung Cell Mol. Physiol. 285 (2003) L363–L369.
[36] N.N. Liu, Z.S. Liu, S.Y. Lu, P. Hu, Y.S. Li, X.L. Feng, et al., Full-length cDNA cloning, molecular characterization and differential expression analysis of peroxiredoxin 6 from Ovis aries, Vet. Immunol. Immunopathol. 164 (2015) 208–219.
[37] M. Yasuike, E. Sugaya, Y. Nakamura, Y. Shigenobu, Y. Kawato, W. Kai, et al., Complete genome sequences of Edwardsiella tarda-Lytic Bacteriophages KF-1 and IW-1, Genome Announc. (2013) 1.
[38] K.I. Kim, J.Y. Kang, J.Y. Park, S.J. Joh, H.S. Lee, Y.K. Kwon, Phenotypic traits, virulence-associated gene profile and genetic relatedness of Edwardsiella tarda isolates from Japanese eel Anguilla japonica in Korea, Lett. Appl. Microbiol. 58 (2014) 168–176.
[39] K. Okonechnikov, O. Golosova, M. Fursov, team U. Unipro UGENE: a unified bioinformatics toolkit, Bioinformatics 28 (2012) 1166–1167.
[40] K.J. Livak, T.D. Schmittgen, Analysis of relative gene expression data using real-time quantitative PCR and the 2(-Delta Delta C(T)) Method, Methods 25 (2001) 402–408.
[41] M.M. Bradford, A rapid and sensitive method for the quantitation of microgram quantities of protein utilizing the principle of protein-dye binding, Anal. Biochem. 72 (1976) 248–254.
[42] T. Mosmann, Rapid colorimetric assay for cellular growth and survival: application to proliferation and cytotoxicity assays, J. Immunol. Methods 65 (1983) 55–63.
[43] H. Sauri, L. Butterfield, A. Kim, H. Shau, Antioxidant function of recombinant human natural killer enhancing factor, Biochem. Biophys. Res. Commun. 208 (1995) 964–969.
[44] Y.S. Lim, M.K. Cha, H.K. Kim, T.B. Uhm, J.W. Park, K. Kim, et al., Removals of hydrogen peroxide and hydroxyl radical by thiol-specific antioxidant protein as a possible role in vivo, Biochem. Biophys. Res. Commun. 192 (1993) 273–280.
[45] L. Ren, T. Xu, R. Wang, Y. Sun, Miiuy croaker (Miichthys miiuy) Peroxiredoxin2: molecular characterization, genomic structure and immune response against bacterial infection, Fish Shellfish Immunol. 34 (2013) 556–563.
[46] Y. Zhang, I-TASSER server for protein 3D structure prediction, BMC Bioinforma. 9 (2008) 40.
[47] B. Hofmann, H.J. Hecht, L. Flohe, Peroxiredoxins. Biol. Chem. 383 (2002) 347–364.
[48] A. Hamza, Homology modeling and docking mechanism of the mercaptosuccinate and methotrexate to P. falciparum 1-Cys peroxiredoxin: a preliminary molecular study, J. Biomol. Struct. Dyn. 20 (2002) 7–20.
[49] T.H. Lee, S.L. Yu, S.U. Kim, Y.M. Kim, I. Choi, S.W. Kang, et al., Characterization of the murine gene encoding 1-Cys peroxiredoxin and identification of highly homologous genes, Gene 234 (1999) 337–344.
[50] L. Ren, Y. Sun, R. Wang, T. Xu, Gene structure, immune response and evolution: comparative analysis of three 2-Cys peroxiredoxin members of miiuy croaker, Miichthys miiuy, Fish. Shellfish Immunol. 36 (2014) 409–416.
[51] S.H. Ling, X.H. Wang, L. Xie, T.M. Lim, K.Y. Leung, Use of green fluorescent protein (GFP) to study the invasion pathways of Edwardsiella tarda in in vivo and in vitro fish models, Microbiology 146 (Pt 1) (2000) 7–19.
[52] C.S. Yang, D.S. Lee, C.H. Song, S.J. An, S. Li, J.M. Kim, et al., Roles of peroxiredoxin II in the regulation of proinflammatory responses to LPS and protection against endotoxin-induced lethal shock, J. Exp. Med. 204 (2007) 583–594.
[53] G.H. Kaihami, J.R. Almeida, S.S. Santos, L.E. Netto, S.R. Almeida, R.L. Baldini, Involvement of a 1-Cys peroxiredoxin in bacterial virulence, PLoS Pathog. 10 (2014) e1004442.
[54] B.M. Gallagher, S.A. Phelan, Investigating transcriptional regulation of Prdx6 in mouse liver cells, Free Radic. Biol. Med. 42 (2007) 1270–1277.
[55] D. Yang, Y. Song, X. Wang, J. Sun, Y. Ben, X. An, et al., Deletion of peroxiredoxin 6 potentiates lipopolysaccharide-induced acute lung injury in mice, Crit. Care Med. 39 (2011) 756–764.
[56] D.L. Borjesson, S.D. Kobayashi, A.R. Whitney, J.M. Voyich, C.M. Argue, F.R. Deleo, Insights into pathogen immune evasion mechanisms: Anaplasma phagocytophilum fails to induce an apoptosis differentiation program in human neutrophils, J. Immunol. 174 (2005) 6364–6372.
[57] L. Alexopoulou, A.C. Holt, R. Medzhitov, R.A. Flavell, Recognition of double-stranded RNA and activation of NF-kappaB by Toll-like receptor 3, Nature 413 (2001) 732–738.
[58] M.L. Reshi, Y.C. Su, J.R. Hong, RNA viruses: ROS-mediated cell death, Int. J. Cell Biol. 2014 (2014) 467452.
[59] D.L. Sutton, G.H. Loo, R.I. Menz, K.A. Schuller, Cloning and functional characterization of a typical 2-Cys peroxiredoxin from southern bluefin tuna (Thunnus maccoyii). Comparative biochemistry and physiology Part B, Biochem. Mol. Biol. 156 (2010) 97–106.
[60] A. Kumin, C. Huber, T. Rulicke, E. Wolf, S. Werner, Peroxiredoxin 6 is a potent cytoprotective enzyme in the epidermis, Am. J. Pathol. 169 (2006) 1194–1205.
[61] Y. Manevich, T. Sweitzer, J.H. Pak, S.I. Feinstein, V. Muzykantov, A.B. Fisher, 1-Cys peroxiredoxin overexpression protects cells against phospholipid peroxidation-mediated membrane damage, Proc. Natl. Acad. Sci. U. S. A. 99 (2002) 11599–11604.
[62] I. Banmeyer, C. Marchand, A. Clippe, B. Knoops, Human mitochondrial peroxiredoxin 5 protects from mitochondrial DNA damages induced by hydrogen peroxide, FEBS Lett. 579 (2005) 2327–2333.
[63] K. Kim, I.H. Kim, K.Y. Lee, S.G. Rhee, E.R. Stadtman, The isolation and purification of a specific "protector" protein which inhibits enzyme inactivation by a thiol/Fe(III)/O2 mixed-function oxidation system, J. Biol. Chem. 263 (1988) 4704–4711.
[64] Y. Luo, E.S. Henle, S. Linn, Oxidative damage to DNA constituents by iron-mediated fenton reactions. The deoxycytidine family, J. Biol. Chem. 271 (1996) 21167–21176.